RESEARCH

Study on deep learning methods for coal burst risk prediction based on mining-induced seismicity quantification

Xianggang Cheng · Wei Qiao · Hu He

© The Author(s) 2023

Abstract The assessment of Coal burst risk (CBR) is the premise of bump disaster prevention and control. It is the implementation criterion to guide various rock burst prevention and control measures. The existing static prediction and evaluation methods for CBR cannot be effectively combined with the results of underground dynamic monitoring. This study proposed a mining-induced seismicity information quantification method based on the fractal theory. Deep learning methods were used to construct a deep learning framework of coal burst risk (DLFR) based on the fractal dimension of microseismic information. Gray correlation analysis (GRA), information gain ratio (IGR), and Pearson correlation coefficient are used to screen and compare factors. Statistical evaluation indicators such as macro-F1, accuracy rate, and fitness curve were used to evaluate model performance. Taking the Gaojiapu coal mine as a case study, the performance of deep learning models such as BP Neural Network (BP), Support Vector Machine (SVM) and its optimized model based on particle swarm optimization (PSO) algorithm under this framework is discussed. The research results' reliability and validity are verified by comparing the predicted results with the actual results. The research results show that the prediction results of CBR in DLFR are consistent with the actual results, and the model is reliable and effective. The mining-induced seismicity quantification can solve the problem of insufficient training samples for the CBR. With this, different pressure relief measures can be formulated based on the results of the CBR predictions to achieve "graded" precise prevention and control.

Highlights

- Method to quantify mining-induced microseisms based on the Fractal theory.
- A deep learning framework for coal burst risk prediction.
- A new method for static predicting and evaluating the risk of coal burst areas was proposed.

1 Introduction

The geodynamic disasters induced by human beings during the construction of deep underground space

X. Cheng (✉) · W. Qiao (✉) · H. He
School of Resources and Geosciences, China University of Mining and Technology, 1 Daxue Road, Xuzhou 221116, Jiangsu, People's Republic of China
e-mail: xgcheng@cumt.edu.cn

W. Qiao
e-mail: qiaowei@cumt.edu.cn

🖄 Springer

utilization and deep mineral resource mining have been the focus of global research for nearly a hundred years (Borisov et al. 2019). Coal bursts and mining-induced seismicity are typical geodynamic disasters, often causing severe damage to shafts and roadways and heavy casualties (Cao et al. 2023; Cheng et al. 2023). Coal bursts have occurred in coal mines in over 20 large coal mining countries, including South Africa, Germany, Canada, Russia, and Australia (Wu et al. 2022). On May 12, 2014, a coal burst accident occurred at a coal mine in Boone County, West Virginia, USA, killing two miners (Newman and Newman 2021). Coincidentally, on May 24, 2020, a coal burst accident happened at the Mengcun coal mine in Shaanxi Province, China, injuring six miners. The assessment of coal burst risk (CBR) is the premise of coal burst disaster prevention and the implementation criterion to guide various coal burst prevention and control measures (Dou et al. 2018; Dai et al. 2022). Accurate coal burst prediction is critical for high-efficiency mine production and ensures the life safety of underground workers.

Research on CBR assessment methods in coal mines mainly focuses on dynamic monitoring and early warning (DMEW) as well as static prediction and evaluation of CBR (Dou et al. 2022). The DMEW method largely uses practices such as drilling cuttings, mine-pressure measurements, microseismic, ground sound, and electromagnetic radiation monitoring (Jiang et al. 2016; Cai et al. 2020; Duan et al. 2021). These methods are affected by the scope of underground mining activities and are suitable for real-time dynamic early warning of coal burst hazards in the production stage. The static evaluation of coal burst risk is widely used in the mine design and development preparation stage.

Numerous studies have been completed on the static prediction and evaluation of CBR in recent years. Dou and He (2002) statistically analyzed the cases of coal burst mines in China. They proposed a comprehensive index method for the prediction of CBR by using mining and geological factors such as Coal seam thickness (CST), Mining depth (MD), Elastic energy index, the Ratio of stress increment caused by the structure to the standard stress value (RIS), and rock-layer thickness characteristic parameter (RTP). Bukowska (2006) studied the Upper Silesia Coal Basin and proposed an assessment system of the CBR based on seven natural conditions of

mining operations. Peng et al. (2010) analyzed the mechanism of coal bursts and, taking the bursting liability and stress state of coal as the influencing factors of the CBR, proposed a simple CBR assessment method. Zhang et al. (2016a, b) used the geodynamic zoning method to analyze active regional faults, dividing the fault block structure of active faults at all levels. They proposed an evaluation method for CBR based on fault structure and coal-rock characteristics. Konicek and Schreiber (2018) analyzed typical examples of coal bursts recorded in the Czech part of the Silesian Coal Basin in rock mass protection pillars, using microseismic activity recorded during longwall mining to roughly assess the CBR in coal mines. Zhu et al. (2018) analyzed the relationship between coal burst and five factors: MD, tectonic stress, vertical crustal movement, active fault, and roof hard rock ratio. They established an assessment model for the CBR using AHP (Analytic Hierarchy Process) and a fuzzy comprehensive evaluation method. Zhang et al. (2022) used the LS-FAHP-CRITIC method to evaluate the CBR in mining areas by combining five indicators: CST and MD, initial in-situ stress, geological structure, and sedimentation. Du et al. (2022) selected microseismic monitoring signals as critical indicators, establishing a normal distribution function of microseismic daily frequency, and proposed a quantitative evaluation method for CBR.

Although the above studies have promoted the development of CBR assessment, there are still several issues. First, many factors affect coal bursts, and there is a deep coupling between each factor Qi et al. (2019). Based only on the geological and mining information before mining, the qualitative classification and evaluation of CBR in mines and local areas are highly subjective and unreliable. Second, the existing static prediction methods with dynamic monitoring and early warning methods are independent. Some data are ignored, and there are still significant errors in the actual comparison to prediction results. Applying the results of dynamic monitoring to the static prediction and evaluation of CBR is critical research.

This study proposes a method for quantifying mining-induced seismicity information based on the fractal theory. A deep learning framework of coal burst risk (DLFR) based on the fractal dimension of dynamic monitoring information is constructed using the deep learning method. Using the

Gaojiappu Coal Mine as an example, a prediction of CBR is carried out based on the DLFR. During the modelling process, the gray relational analysis (GRA), information gain ratio (IGR), and Pearson correlation coefficient are used to screen the model factors to gain more representative samples and improve the model accuracy. Finally, the model performance is evaluated using statistical evaluation indicators such as macro-F1 (macro-F1), accuracy rate (ACC), and fitness curve. Conduct a comparative analysis between the predicted results of a study area and the actual field results through a specific case study to validate the reliability of research findings. The performances of deep learning models are discussed, such as BP, SVM, PSO-BP, and PSO-SVM, under this framework, aiming to establish a stable and high-quality CBR identification model and provide some inspiration for the research on CBR assessment methods. According to the results of CBR identification, a "graded" precise pressure relief design can be performed, providing the basis and guidance for the design of coal mine coal burst prevention and control.

1.1 Geological setting

The Gaojiapu coal mine is located in the plateau area in the southwest Ordos Basin, primarily a beam and gully landform. The length and width of the coal mine are 25.7km and 16.6km, respectively, and the minefield area is 219.16 km^2 (Fig. 1a). The mine uses the vertical shaft development method, and the underground coal mining method consists of longwall coal mining of mainly the No.4 coal seam of the Jurassic Yan'an Formation. Currently, the research area is divided into three panels for mining. Due to the coal burst disaster impact, the first-panel subsequent working face is not mined. The second-panel has been fully extracted, and the third-panel area is designated as the continuous production area. The research area has installed a new 'SOS' microseismic monitoring system designed and manufactured by the Polish Institute of Mine Research. The system is capable of Real-time dynamic monitoring of microseismic signals with energy greater than 100J in the study area. It can accurately calculate the energy, time, and location of mining-induced microseismicity (Kan et al.
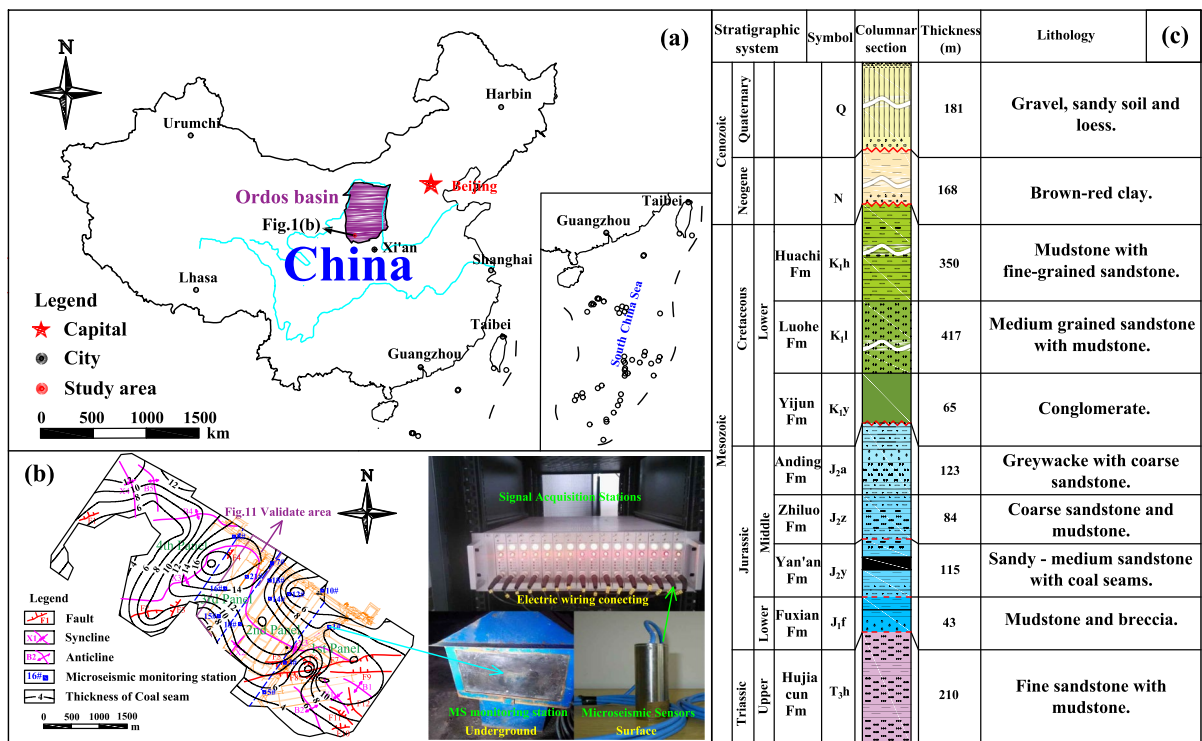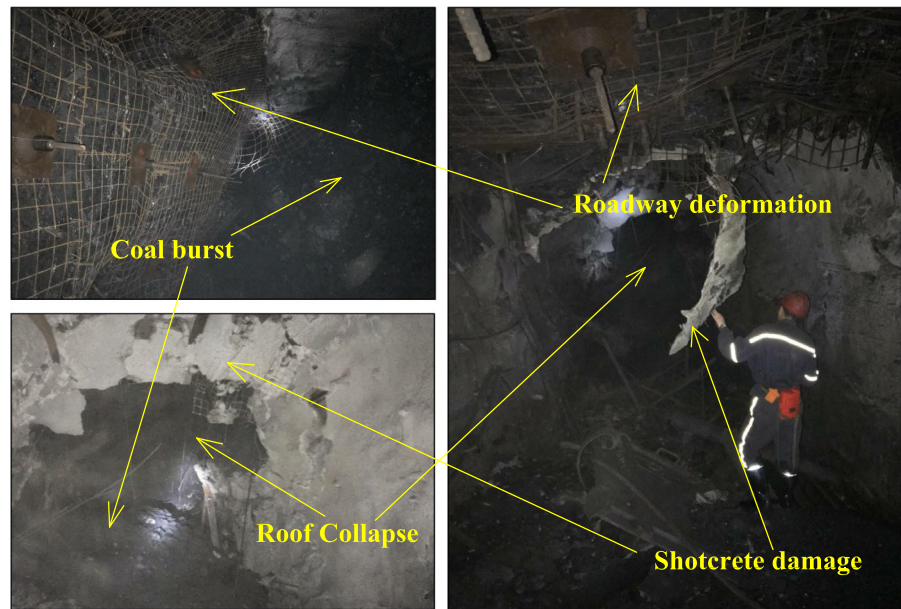

Fig. 1 Location of the study area and layout of microseismic monitoring sensors

Fig. 2 Photos showing severe coal burst in the study area

2022). The sensor installation position of this monitoring system is shown in Fig. 1b. By collecting all the microseismic monitoring data in the study area since installing the 'SOS' microseismic monitoring system. Due to the complex geological conditions of the study area, the geodynamic hazards are highly active. Because of coal extraction, numerous coal burst accidents have occurred, seriously affecting the safety of mine production (Fig. 2).

1.2 Coal burst affecting factors

Based on an extensive literature survey, field survey analysis, and previous work, the previous coal burst prediction included the following factors (Dou and He 2002; Sun et al. 2021; Zhu et al. 2018): CST, coal seam dip angle, MD, roof lithology, elastic energy (W), structural conditions, maximum tangential stress, uniaxial compressive strength (Uc), ratio of stress increment caused by the structure to the standard stress value (RIS), and rock-layer thickness parameter (RTP). In this study, 11 factors, both qualitative and quantitative, were selected, namely coal seam thickness (CST), mining depth (MD), rock-layer thickness parameter (RTP), thickness of overburden hard rock-layer and its spacing with the coal seam, sedimentary characteristics of roof strata, rock mass quality evaluation score (RQS), geological structural capacity dimension (GSD),

RIS, lateral pressure coefficient (LPC), and elastic energy (W). Table 1 shows the source of each factor selection and its significance.

In China's coal burst prevention and control standards, RTP within 100 m of the roof is used as an evaluation indicator. However, due to the development of the Jurassic Coalfield and the change in coal mining technology, the range of the mining deformation and damage disturbance zone is more extensive than that of the previous mining projects (Han et al. 2023). Therefore, this study selected an RTP within 200 m of the roof as the evaluation factor. According to the geological data of the Gaojiapu coal mine, there are three widely distributed hard sandstone strata on the roof layer (Fig. 1c). Therefore, a total of 6 groups of information on the thickness of overburden hard rock-layer and its spacing with the coal seam were used to reflect the impact of the roof hard rock layer on coal explosion (Fig. 3d–i). Besides, based on the tectonic evolution history, the overburden sedimentary microfacies of the study area were divided into three levels by the sedimentary discontinuity as the dividing line, namely the Yan'an Formation sedimentary microfacies (YS) (Fig. 3j), the Zhiluo and Anding Formations sedimentary microfacies (ZAS) (Fig. 3k), and the Luohe Formation sedimentary microfacies (LS) (Fig. 3l). Finally, 17 pieces of information out of 11 factors were selected in this Study (Fig. 3).

Table 1 Influencing factors of coal burst and its significance

Factors	Significance
Coal seam thickness (CST)	The intensity of underground coal mining (Sun et al. 2021)
Mining depth (MD)	The stress level of the surrounding rock in the coal mine (Sun et al. 2021)
Rock-layer thickness parameter (RTP)	The ability of the overlying rock to store and release elastic energy (Dou and He 2002)
Thickness of overburden hard rock-layer and its spacing with the coal seam	The hard strata in the overlying rock is closely related to the occurrence of geodynamic disasters such as coal bursts (Kuang et al. 2019)
Sedimentary characteristics of roof strata	The sedimentary characteristics of the roof strata that define the basic environment of coal burst disasters (Zhang et al. 2022)
Rock mass quality evaluation score (RQS)	The quality and stability of engineering geological rock mass (Zhang et al. 2016a, b)
Geological structural capacity dimension (GSD)	Quantitatively evaluate the complexity of geological structures and reflect the distribution and development characteristics of geological structures (Qiao et al. 2019; Zhou et al. 2022)
Ratio of stress increment caused by the structure to the standard stress value (RIS)	The degree of structural stress concentration (Dou and He 2002). It is usually used for estimation when there are no measured values of in-situ stress
Lateral pressure coefficient (LPC)	It represents the stress state and reflects the accumulation, release and deformation mode of rock mass energy (Cheng et al. 2023)
Elastic energy (W)	The size of elastic strain energy accumulation in the state of the natural in-situ stress field (Wang and Cui 2018)

2 Methodology

### 2.1 Deep learning framework of coal burst risk (DLFR)

With the rapid development of computational simulation and deep learning technology, deep learning-assisted geoscience mining has shown good application prospects (Ma and Mei 2021). Many studies use deep learning technology to provide effective paths and solutions for solving geological problems (Polson and Sokolov 2020). This study constructed a deep learning framework of coal burst risk (DLFR) based on the fractal dimension of microseismic information. The risk identification of coal bursts was performed as shown in Fig. 4. First, based on the fractal theory, the mining-induced seismicity information data of underground monitoring were quantified. A CBR database was established for the study area through statistical analysis of mine geological data. Then, the collinearity diagnosis and screening of factors were performed through the GRA, Pearson correlation coefficient, and IGR. This enables more representative samples and improved model accuracy. Statistical evaluation metrics such as macro-F1, ACC, and fitness curve were used to evaluate model performance, and the performances of deep learning models such as

BP, SVM, PSO-BP, and PSO-SVM under the DLFR were discussed. Finally, conduct a comparative analysis between the predicted results of a study area and the actual field results through a specific case study to validate the reliability of research findings.

2.2 Fractal quantification method of mining-induced seismicity

Fractal geometry was first proposed in the 1960s to describe complex natural shapes (King 1983). The fractal theory is widely used in various disciplines such as mathematics, physics, biology, economics, and geology (Turcotte 1986). The location and area where microseismic events occur have a self-similarity system, which is the same as the geological structures and has statistical similarity in geometry. The microseismic monitoring signal can be used as a parameter to comprehensively reflect the risk of coal burst (Si et al. 2020; Wang et al. 2022). In this paper, fractal research on the distribution characteristics of microseismic events was performed through the fractal dimension to obtain the fractal quantitative evaluation of coal burst risk.

Assuming that the plane distribution of microseismic events is a fixed point set A contained in a rectangle, it can be divided into several grids with side
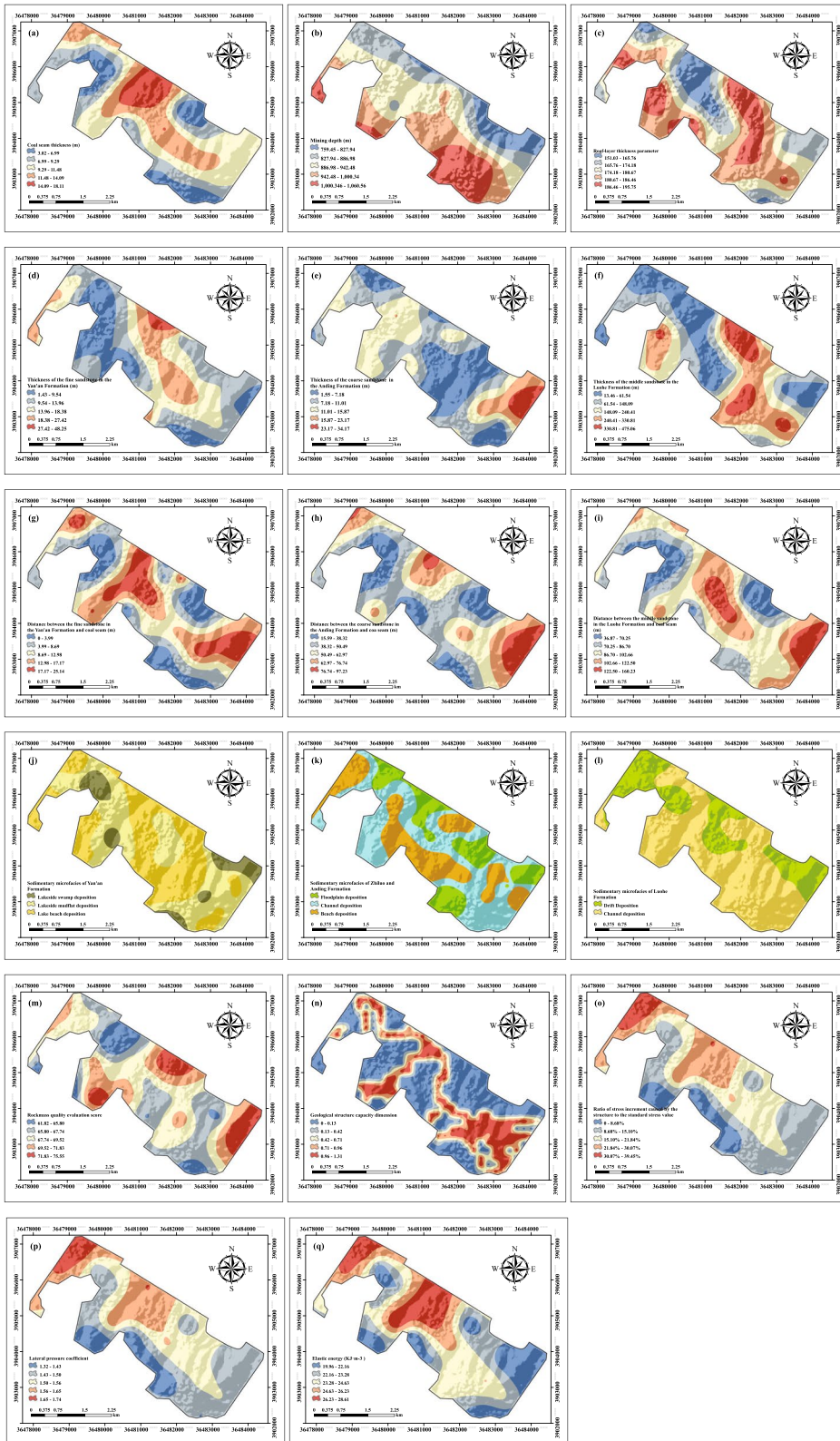
◄**Fig. 3** Spatial distribution of each factor in the study area (a-q). **a** Coal seam thickness. **b** Mining depth. **c** Roof-layer thickness parameter. **d** Thickness of the fine sandstone in the Yan'an Formation. **e** Thickness of the coarse sandstone in the Anding Formation. **f** Thickness of the middle sandstone in the Luohe Formation. **g** Distance between the fine sandstone in the Yan'an Formation and coal seam. **h** Distance between the coarse sandstone in the Anding Formation and coa seam. **i** Diatance between the middle sandstone in the Luohe Formation and coal seam. **j** Sedimentary microfacies of Yan'an Formation. **k** Sedimentary microfacies of Zhiluo and Anding Formation. **l** Sedimentary microfacies of Luohe Formation. **m** Rockmass quality evaluation score. **n** Geological structure capacity dimension. **o** Ratio of stress increment caused by the structure to the standard stress value. **p** Lateral pressure coefficient. **q** Elastic energy.

length a (Velandia and Bermúdez 2018). The distribution points of microseismic events are covered with grids with side length a, and the number of grids containing microseismic events $N(a)$ is recorded. The grid size a_i is continuously reduced to obtain the corresponding grid number $N(a_i)$. A curve can be obtained in the $\ln a$-$\ln N(a)$ coordinate system, and the slope of the straight line segment is the capacity dimension Dms of the distribution of microseismic events in the rectangle (Fig. 5), reflecting the complexity of the distribution of microseismic events in the rectangular area. Dms is calculated as follows:

$$D_{ms}(A) = \lim_{a \to 0} \frac{\ln N(a)}{\ln(a^{-1})} = -\lim_{a \to 0} \frac{\ln N(a)}{\ln a} \tag{1}$$

2.3 Deep learning method

2.3.1 SVM

SVM is a deep learning method suitable for small, non-linear samples with high-dimensional numbers. It was studied and proposed by Vapnik et al. in the
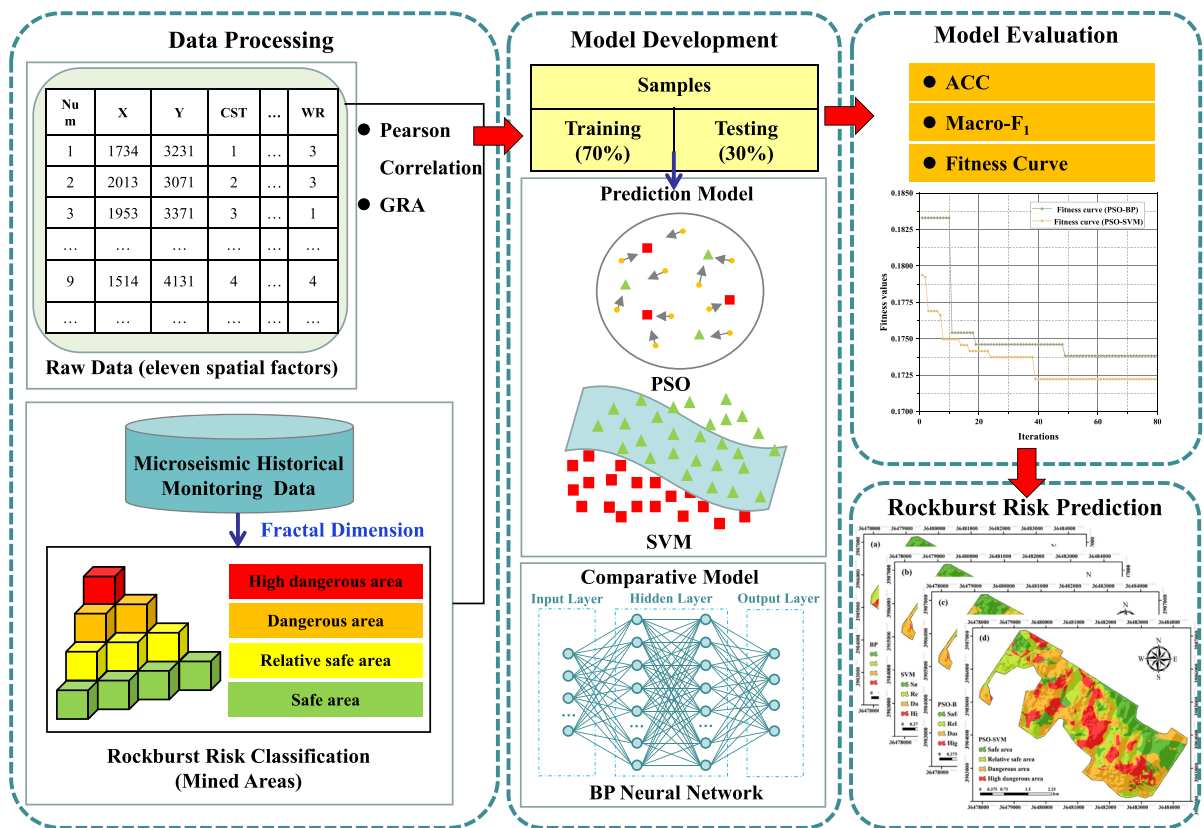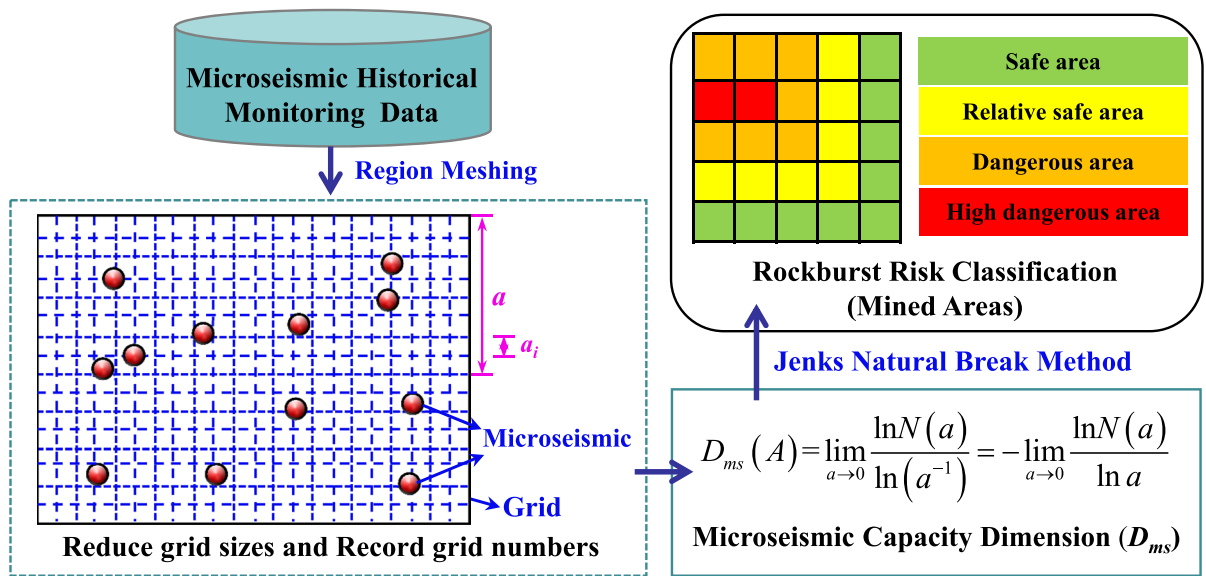

Fig. 4 Flowchart of this study

Fig. 5 Flowchart of mining-induced seismicity fractal quantification method

1970s (Cherkassky and Ma 2004). It is widely used in imaging, biological information, and other information recognition, classification, and regression technologies (Dou et al. 2020). For two-dimensional linear binary classification problems, the optimal classification line becomes the optimal classification surface after being extended to high-dimensional space (Wu et al. 2013). Assuming that the sample set $D = \{(x_i, y_i), \quad i = 1, 2, \dots n\}$, $y_i = \{-1, 1\}$ is linearly separable, its classification surface equation is:

$$[(w \cdot x_i) + b] - 1 \geq 0, \quad i = 1, 2, \dots, n \qquad (2)$$

$$w \cdot x + b = 0 \qquad (3)$$

where y_i is the category label.

Using the Lagrangian function $L(w, \alpha_i, b) = \frac{1}{2}\|w\|^2 - \sum_{i=1}^{n} \alpha_i \{y_i[(w \cdot x_i) + b] - 1\}$ to transform the above formula into a dual problem is as follows:

$$\max \sum_{i=1}^{n} \alpha_i - \frac{1}{2} \sum_{i,j=1}^{n} \alpha_i \alpha_j y_i y_j (x_i \cdot x_j) \qquad (4)$$

$$\text{s.t.} \sum_{i=1}^{n} \alpha_i y_i = 0, \alpha_i \geq 0, i = 1, 2, \dots, n \qquad (5)$$

The kernel function can replace the transformation of the high-dimensional space, and the inner product operation between the sample set data can be processed to determine the optimal classification surface in the high-dimensional space (Liu et al. 2011). The Gaussian Radial Basis Function (RBF) is the most commonly used kernel function and can analyze non-linear data. The optimal classification function is as follows:

$$f(x) = sgn\left(\sum_{i=1}^{n} \alpha_i y_i K(x_i \cdot x) + b\right) \qquad (6)$$

2.3.2 BP

Artificial neural networks (ANN) are divided into two types of network structures: feed-forward neural networks and feedback neural networks (Sun et al. 2015). The backpropagation (BP) method is the core part of the feed-forward neural network, solving non-linear optimization problems through the input and output of a set of samples. Any non-linear function can be approximated with arbitrary precision by adjusting the BP connection weights and network size (including n, m, and the number of hidden layer

neurons) (Liu et al. 2021). The non-linear relationship between the coal burst risk being inverted and a set of neural networks describes the impact factors $(n, h_1, \ldots, h_p, m)$ as follows:

$$\begin{cases} NN(n, h_1, \ldots, h_p, \ m) : R_n \rightarrow R_m \\ D = NN(n, h_1, \ldots, h_p, \ m)(P) \\ P = (p_1, p_2, \ldots, p_n) \ D = (d_1, d_2, \ldots, d_n) \end{cases} \quad (7)$$

where $P = (p_1, p_2, ..., p_n)$ is the input node expression of the neural network, $D = (d_1, d_2, \ldots, d_n)$ is the output node expression of the neural network, $NN(n, h_1, \ldots, h_p, \ m)$ is the established multi-layer neural network structure, and $n, h_1, \ldots, h_p, \ m$ are the node's number of neural networks.

2.4 Particle swarm optimization (PSO)

PSO is a method to solve optimization problems by simulating the process of bird foraging. In particle swarm optimization, birds are abstracted as a group of random particles, and the optimal solution is found through iteration (Zhao et al. 2015). A particle can find the optimal position P_b by itself and identify the optimal position $P_{b,g}$ found by other particles in the entire population. Particles update their position by tracking two optimal solutions (i.e., P_b, $P_{b,g}$) calculated according to the following (Li and Wei 2021):

$$\begin{cases} V_i(t+1) = wV_i(t) + c_1 r_1 [P_{b,i}(t) - x_i(t)] + c_2 r_2 [P_{b,gi}(t) - x_i(t)] \\ x_i(t+1) = x_i(t) + V_i(t+1) \end{cases} \quad (8)$$

where $V_i(t)$ and $x_i(t)$ are the time t's speed and positions of particle i, respectively. c_i is the learning factors and w is the inertia factor. r_1 and r_2 are random numbers in [0, 1].

2.5 Factor screening metrics

2.5.1 GRA

GRA is a method for quantitatively describing and comparing the development and changes of an overall system. According to the geometric similarity of the time series curves of each relevant factor, the relationship between the factors is close, reflecting the degree of correlation between the indicators (Yan and

Li 2013). To eliminate the impact of the non-uniform dimensions of each factor on the results, range transformation is used to perform dimensionless processing on the characterization sequence Y and the impact sequence X. The correlation degree between each component of each sequence is calculated as follows (Wu et al. 2005):

$$\xi(x_0(k), x_i(k)) = \frac{\min\limits_{i} \min\limits_{k} |x_0(k) - x_i(k)| + \rho \max\limits_{i} \max\limits_{k} |x_0(k) - x_i(k)|}{|x_0(k) - x_i(k)| + \rho \max\limits_{i} \max\limits_{k} |x_0(k) - x_i(k)|} \quad (9)$$

$$r(X_0, X_i) = \frac{1}{n} \sum_{k=1}^{n} \xi(x_0(k), x_i(k)) \quad (10)$$

$$Y = X_0 = (x_0(1), x_0(2), ..., x_0(k)) \quad (11)$$

$$X = \begin{bmatrix} x_1(1) & \cdots & x_1(k) \\ \vdots & \ddots & \vdots \\ x_n(1) & \cdots & x_n(k) \end{bmatrix} \quad (12)$$

where $x_0(m)$ is the m-th feature index of Y, $x_i(k)$ is the k-th factor of the i-th component in X, $i = 1, 2, \ldots, n$, $k = 1, 2, \ldots, m$. X', Y' are X, Y dimensionless series, respectively. r is the degree of correlation, ξ is the correlation coefficient, n is the number of samples, i is the number of sub-factors, k is the k-th group of samples, $|x_0(k) - x_i(k)|$ is the absolute value of the sequence X_0 and X_i at the point k, ρ is the resolution coefficient, and the value range is (0, 1).

2.5.2 IGR

Information gain (IG) represents the uncertainty-reduced value of categorical feature M by knowing the information of feature N. It is used to measure the ability of feature N to distinguish datasets (Shen et al. 2022). If there are more feature values, IG is greater. Therefore, only using IG to evaluate the composition of a sample set is not objective enough (Yao et al. 2022). The IGR only offsets the complexity of the feature variables and avoids the existence of over-fitting. IGR is calculated as follows:

$$IGR(M|N) = \frac{g(M|N)}{H_x(M)} \quad (13)$$

where $H(Y|X)$ is the IG of M by given N condition, $g(Y|X)$ is the information gain entropy corresponding to feature N, and $H_x(Y)$ is the information entropy of M about feature N.

2.6 Model performance evaluation metrics

Model performance evaluation is key to predictive models (Yang et al. 2023). In binary classification model evaluation, several commonly used statistical parameters are precision (P), recall (R), and accuracy(ACC). By comparing actual markers with predicted markers, true negatives (TN), true positives (TP), false negatives (FN), and false positives (FP) are determined (Dao et al. 2020). For multi-classification problems, the P and R of different categories are different. Here, evaluation parameters such as macro precision (macro-P), macro recall (macro-R), and macro F1 (macro-F_1) are introduced to determine the performance of the entire model. The formulas for calculating the above evaluation parameters are as follows (Sharma and Kaur 2021):

$$P = \frac{TP}{TP + FP} \tag{14}$$

$$R = \frac{TP}{TP + FN} \tag{15}$$

$$macro - P = \frac{1}{n} \sum_{i=1}^{n} P_i \tag{16}$$

$$macro - R = \frac{1}{n} \sum_{i=1}^{n} R_i \tag{17}$$

$$macro - F_1 = \frac{2 \cdot macro - P \cdot macro - R}{macro - P + macro - R} \tag{18}$$

$$ACC = \frac{TP + TN}{TP + FP + TN + FN} \tag{19}$$

Furthermore, in the PSO optimization model, the fitness function is one of the main concepts used to evaluate the quality or fitness of each particle's solution. The fitness function evaluates the solution quality and judges the model's optimal solution or a solution close to the optimal solution.

3 Results

3.1 Influencing factor screening

First, the correlation between each influencing factor is compared with CBR, and the GRA is used to calculate the correlation degree. The results show that the correlation degree between each influencing factor with CBR is above 0.65, which has a good correlation and can fully indicate the risk of coal burst. Secondly, Pearson correlation analysis was used to determine the correlation among the various factors. When the absolute value of the correlation coefficient of the two factors is greater than 0.7, the relationship is very close (Arndt et al. 1999; Yao et al. 2022)**.** The results of Pearson correlation analysis are shown in Fig. 6. The distance between the medium sandstone strata of the Luohe Formation and coal seam (DLSC) and CST, as well as the LPC and RIS, all show a high correlation (R values are 0.78 and 1, respectively). Finally, the IGR is used to compare the sensitivity of each influencing factor to the CBR and rank the importance of each factor (Fig. 7). The greater the IGR, the greater the information content of the index. Each factor positively contributes to varying degrees (IGR > 002). Among them, compared with DLSC, the IGR of CST is relatively small. Hereby, factor removal is performed to reduce data redundancy, and CTS was chosen to be eliminated. In this study, since we inverted the in-situ stress field (Cheng et al. 2023), RIS is essentially the value obtained by subtracting LPC to 1. Therefore, deleting RIS or LPC has no practical significance because RIS has the same IGR as LPC, and the information they contain is the same. In addition, since LPC is frequently used in most research, we retain LPC in this article. After eliminating factors that cause data redundancy, the filtered influencing factors are used to predict CBR.

3.2 Model performance evaluation

Based on the microseismic monitoring results of the mined areas of the first-panel and the second-panel, the fractal and fractal dimension calculations are carried out. Considering that the horizontal positioning error of the 'SOS' microseismic monitoring system is about 20m (Zhou et al. 2020), we select 20m × 20m as the grid size for microseismic fractal quantification.
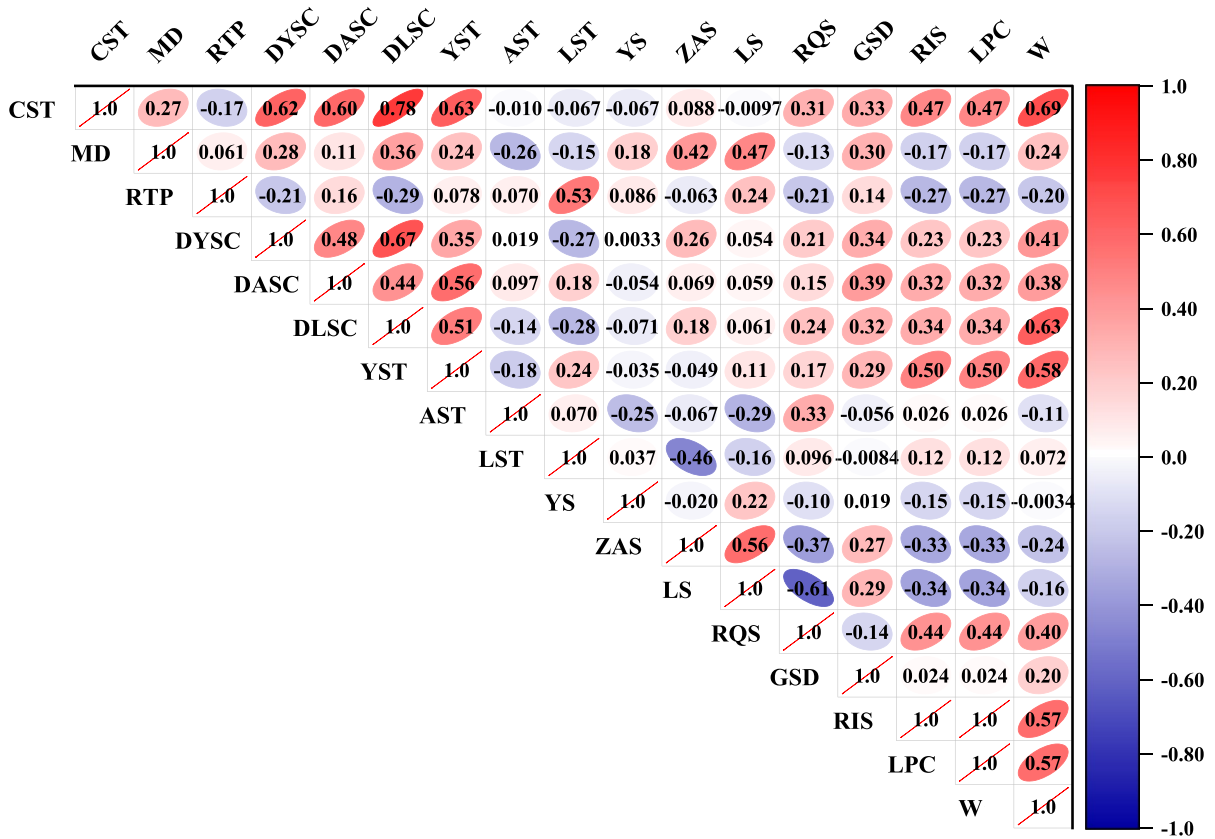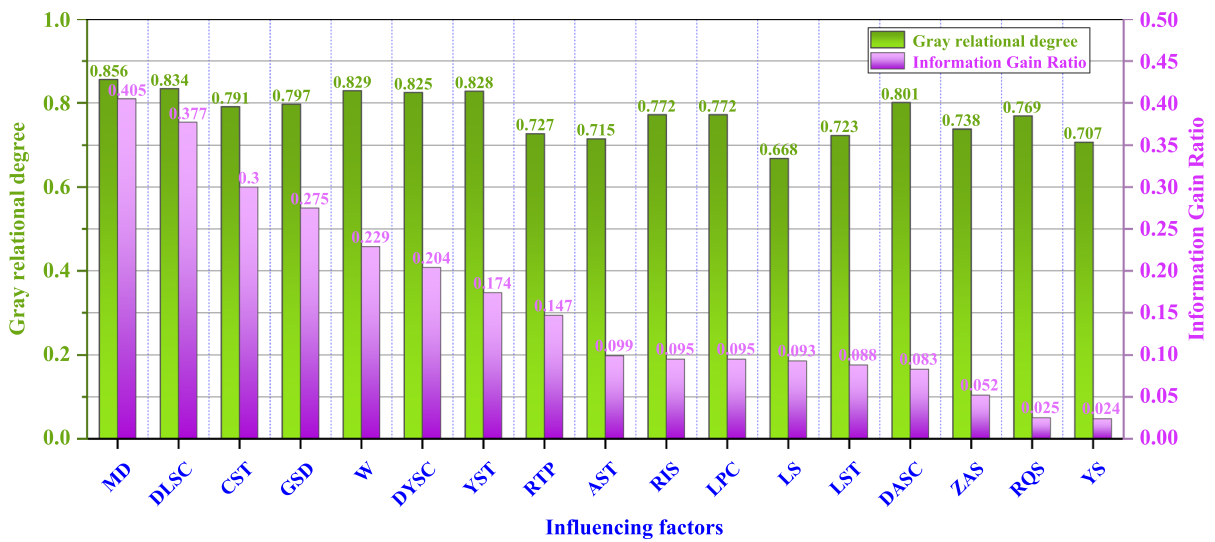
Fig. 6 Pearson correlation coefficient heat map

Fig. 7 Analysis results of gray relational degree and information gain ratio

Table 2 Comparison of model training set metrics

Model	Metrics of training samples			
	Macro-P	Macro-R	Macro-F1	ACC
BP	0.6503	0.6814	0.6655	0.6503
SVM	0.6535	0.6703	0.6618	0.6535
PSO-BP	0.8221	0.8244	0.8233	0.8221
PSO-SVM	0.8661	0.8667	0.8664	0.8661

Table 3 Comparison of model testing set metrics

Model	Metrics of testing samples			
	Macro-P	Macro-R	Macro-F1	ACC
BP	0.6420	0.6679	0.6547	0.6351
SVM	0.6596	0.6800	0.6696	0.6596
PSO-BP	0.7926	0.7968	0.7947	0.7926
PSO-SVM	0.8244	0.8237	0.8240	0.8244

The Jenks natural breaks method divides the monitoring results into four categories: safe area, relatively safe area, dangerous area, and highly dangerous area. The classification results of training samples' risk of coal burst are obtained. Combined with the screened high-purity influencing factor data, a better sample database is obtained for subsequent training and prediction. Seventy percent of the sample data are then randomly selected for model training, and the remaining 30% are for testing the model. The parameters of

the deep learning model are set through past experience and trial and error. The calculation results of model testing indicators are shown in Tables 2, 3, and Fig. 8.

It is worth noting that after the 39th iteration of PSO-SVM, the fitness tends to stabilize, indicating that the model training is the optimal solution. Comparing the results of PSO-SVM and SVM models shows that ACC and Macro-F1 increased by 21.26% and 20.46%, respectively, indicating that the model after PSO optimization has higher accuracy and lower error.

After training the BP neural network model for comparison, the model evaluation index shows that when the SVM model (ACC = 65.35%) is used for the discrimination and classification of this problem, the accuracy is higher than that of the BP neural network model (ACC = 65.03%). The PSO-SVM and PSO-BP model accuracies are 86.61% and 82.21%, respectively, indicating that CBR can be effectively identified under the DLFR in this dataset (Figs. 9, 10).

Although the precision and accuracy of each model after PSO optimization have been significantly improved, the PSO-BP model tends to stabilize after the 48th iteration. The fitness value is also greater than that of the PSO-SVM model. In addition, the ACC and Macro-F1 of the PSO-SVM model are still greater than those of the PSO-BP model, indicating that the PSO-BP model needs a longer time and process to solve the problem. Furthermore, the accuracy
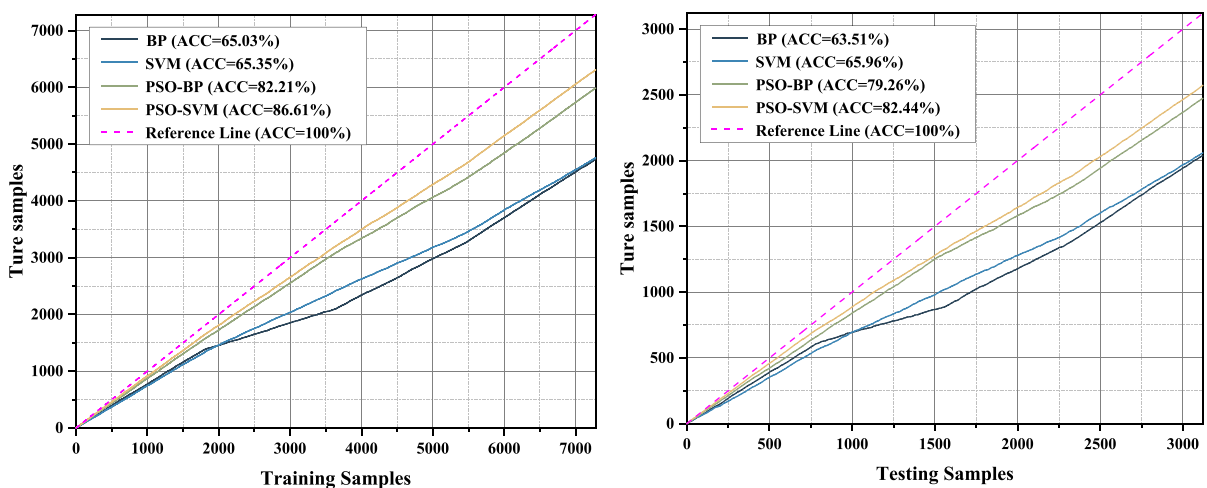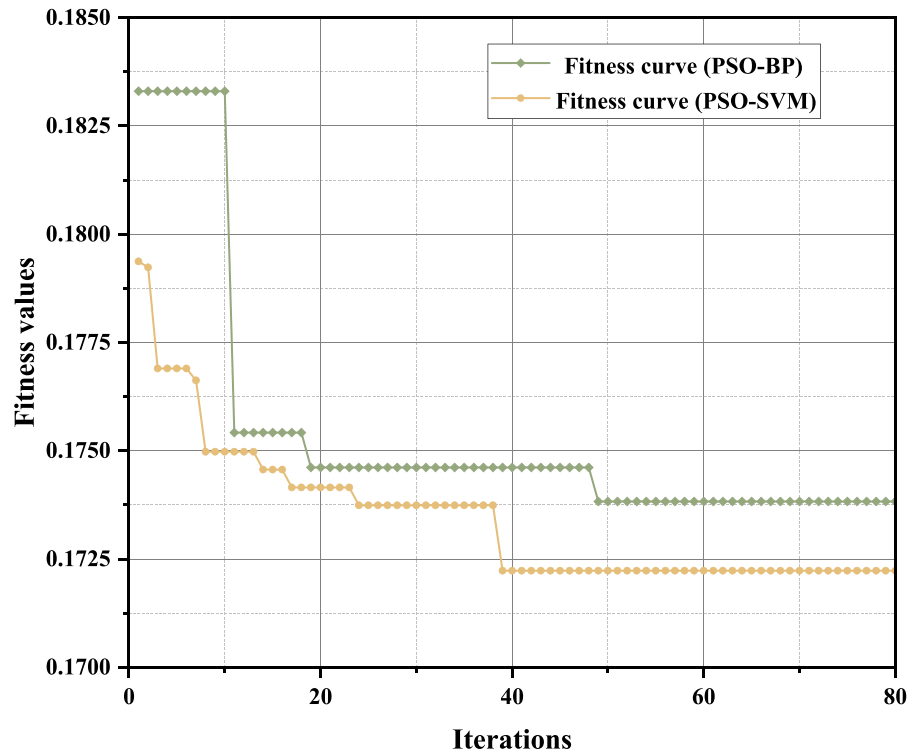

Fig. 8 Time series distribution plot of training and testing samples

Fig. 9 The fitness curve of the PSO optimization model

of the PSO-BP model is not high than that of the PSO-SVM model, indicating that the PSO-SVM model is more significant for solving this problem.

3.3 Model results validation

To further verify the reliability of the research results and methods, a comparative analysis by comparing the high-energy microseismic records and shock manifestations of the 3rd-panel coalfaces. During the mining of the 301 coalface and the 302 coalface, more than 100 high-energy microseismic events of more than 10^3 J occurred. Among them, there are 39 microseismic events greater than 10^4 J and 17 microseismic events greater than 10^5 J, as shown in Fig. 11. In addition, the coal burst phenomena occurred in two areas in the middle of the 301 coalface and near the stop production line, resulting in the sinking of the roof and the drop of the shotcrete layer. From the results of the PSO-BP model and PSO-SVM model in Fig. 11, it can be seen that the microseismic high-energy events during the 3rd-panel mining period are mostly located in the predicted dangerous area and high dangerous area, and the microseismic events greater than 10^3 J are less

distributed in the safe area and relatively safe area. In addition, high-energy microseismics greater than 10^5 J are mostly located in high dangerous area. Especially the area where the coal burst phenomena occurred are also found in high dangerous area. The results show that the prediction results of the model in this study are basically consistent with the actual results, the model and method are reliable and effective, and can be used for coal burst risk prediction and further guidance for field production work.

It is worth noting that the energy of microseismic events in high dangerous area and dangerous area is high. In contrast, the energy of microseismic events in safe area and relatively safe area is low. This also means that strong pressure relief measures need to be developed in high dangerous area and dangerous area to avoid coal bursts. The CBR warning and prevention are complementary. With this, reasonable and effective pressure relief measures are formulated for different CBR levels based on the results of the deep learning predictions to achieve "graded" precise prevention and control. Taking the study area as an example, the "graded" pressure relief suggestions and measures are shown in Table 4.
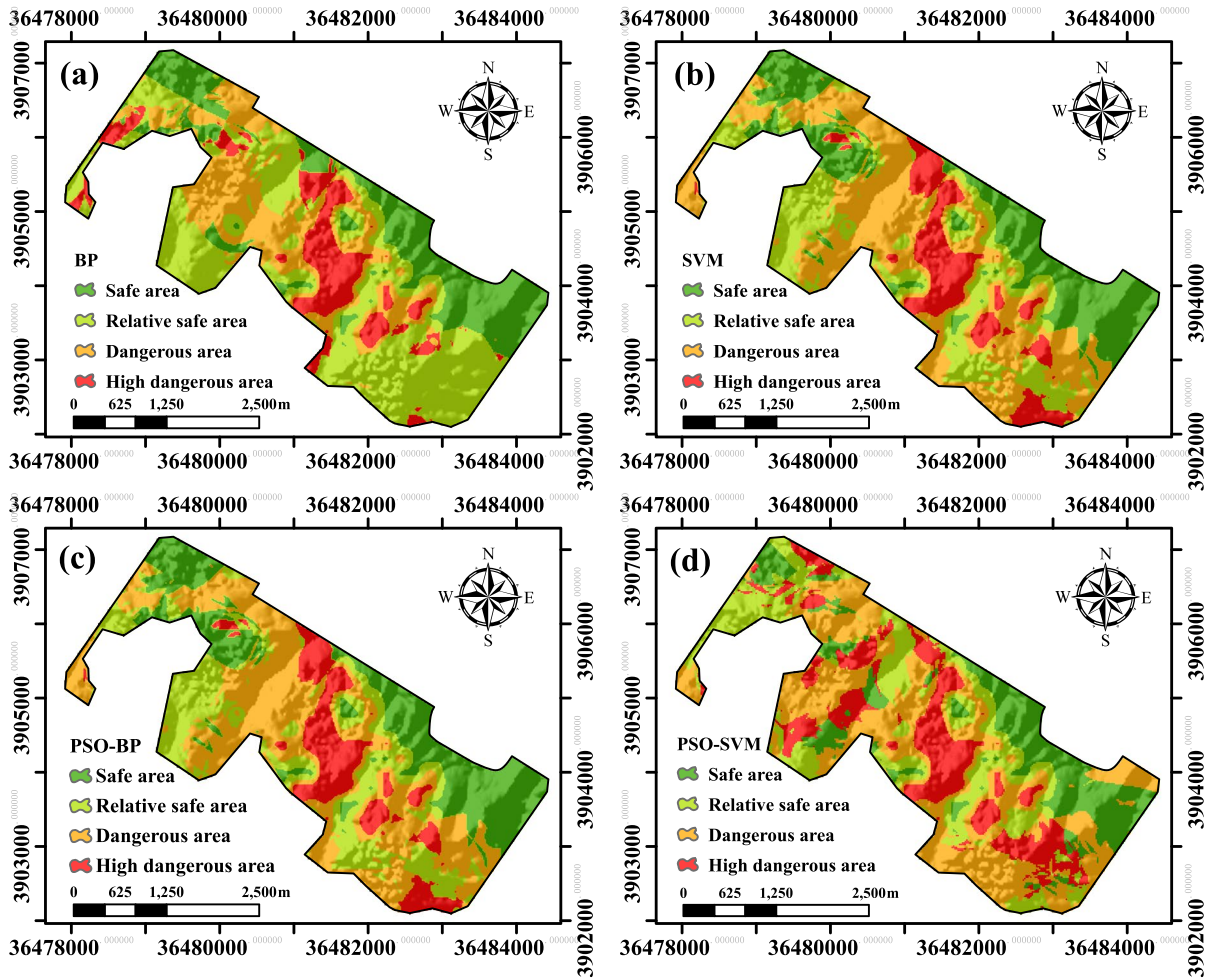
Fig. 10 Prediction results of coal burst risk for each model. **a** BP model. **b** SVM model. **c** PSO-BP model. **d** PSO-SVM model

Fig. 11 Comparison of forecasted results and actual results of 3rd-panel working face. **a** PSO-BP model. **b** PSO-SVM model
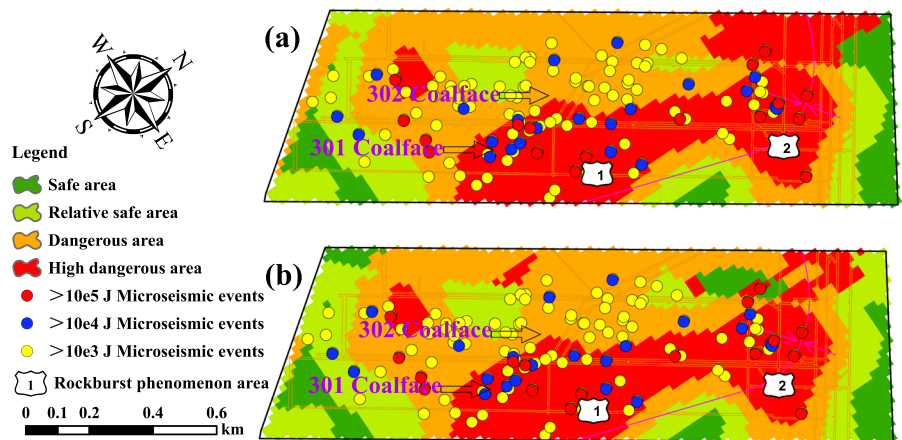
Table 4 "Graded" stress relief suggestions and measures of the study area

Prediction results	Suggestions	Measures to relief stress of the study area
Safe area	Weakening the rock burst tendency and strengthening the monitoring	Multi-parameter microseismic monitoring and early warning
Relative safe area	Pre-pressure relief and strengthening the monitoring	Pressure relief through large-diameter drilling or coal seam blasting
Dangerous area	Strengthening the monitoring and the pressure relief	Take multiple measures to enhance the stress relief effect. (On the basis of pre-pressure relief measures, some other pressure relief measures should be supplemented or enhanced)
High dangerous area	Strengthening the pressure relief and the reinforcing support	Based on pressure relief measures in Dangerous area, the roof was weakened and cutted. Supplementary measures in the study area include deep hole blasting and hydraulic fracturing in the roof

4 Discussion

4.1 Analysis of influencing factors of coal burst

Like other geological disasters, the occurrence of coal bursts is a complex non-linear process affected by numerous factors. This study uses the weighted frequency ratio (FR) in the statistical analysis method to determine the importance of each factor to the highly dangerous area, as shown in Fig. 12. Coal burst high dangerous areas mainly occur in areas with large MD, high W, large LPC, and high GSD. This area's geological environment and tectonic stress are complex and have a high static load. When interacting with small dynamic load disturbances, the critical stress load may be exceeded to induce a coal burst.

Except for depth, GSD and W are positively correlated with the coal burst risk, and the thickness of fine-grained Yan'an Formation sandstone (YST), DLSC, and the distance between the fine-grained Yan'an Formation sandstone and coal seam (DYSC) also have a positive correlation with the coal burst risk to a certain extent. This indicates that the overburden hard rock-layer has a specific influence on the coal burst. Among them, the greater YST and DYSC are, the easier it is to induce coal bursts. On the contrary, the thinner the sandstone strata in the Luohe Formation (LST) and DLSC, the easier it is to induce coal bursts. This indicates that the thickness and spacing of the hard rock formations of the roof must be in the appropriate range to cause a coal burst. This is also confirmed by the Anding Formation coarse-grained sandstone (AST) thickness results and its distance to the coal seam (DASC). This result is also helpful in studying the target layer identification of underground roof fracturing pressure relief technology.
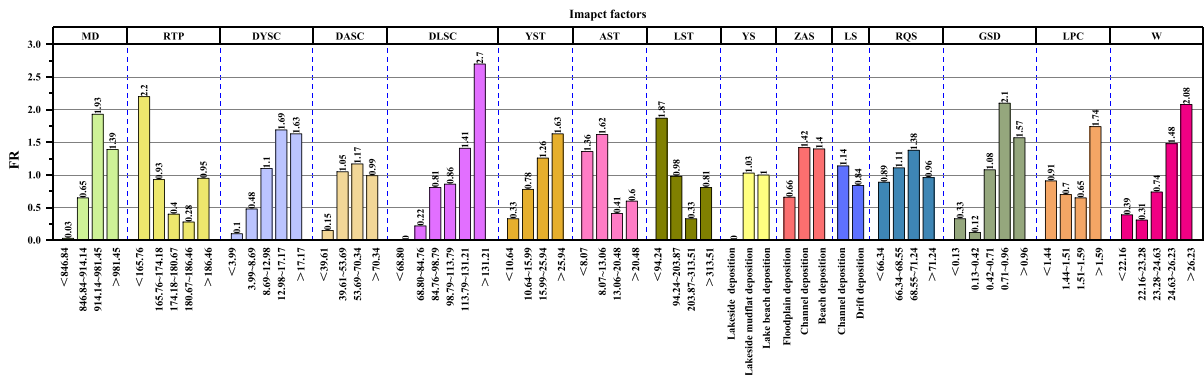

Fig. 12 FR of coal burst influencing factors

It is worth mentioning that RTP and RQS did not show a linear relationship with coal burst hazard. This seems to be inconsistent with previous studies. The smaller the RTP, the easier it is for the roof rock to break under mining conditions. Furthermore, it is easier to generate dynamic loads to induce coal bursts. The results of RQS show that the extremes of roof strata quality adversely affect coal bursts. Because the better the quality of the roof strata, the overburden is difficult to break under mining conditions. However, a poor-quality roof typically has more broken strata, and it is not easy to accumulate a large amount of elastic energy. The sedimentary microfacies of each group of formations show a certain degree of consistency; that is, the depositional environment with strong hydrodynamic conditions is more likely to induce coal burst than the depositional environment with weak hydrodynamic conditions. Finally, when the LPC is high, FR is high, indicating that the CBR is small when the difference in the stress environment is small.

4.2 Performance of deep learning for the CBR prediction

The traditional static prediction method of coal bursts can only be evaluated by fusing qualitative and quantitative multivariate information. Also, its prediction results lack reliability. In this study, the fractal and fractal dimension calculation of the microseismic monitoring results in the mining area is converted into the classification results of CBR. This solves the problem of insufficient coal burst training samples to a certain extent.

This study chose PSO-SVM as the basic model to solve the problem of the CBR's non-linear judgment, improving the model accuracy and reducing data redundancy through factor selection and screening. The effect of the deep learning structure optimized by the PSO algorithm is significantly better than ordinary deep learning. One of the fundamental reasons is that the combined deep learning algorithm can ensure the convergence and accuracy of deep learning and improve the convergence speed of problem-solving. By combining deep learning technology, this study provides a new method for studying coal mine coal burst risk assessment.

5 Conclusions

Based on the fractal theory, this study quantified the mining-induced seismicity information. High-reliability samples were screened out through factor analysis, a deep learning risk identification framework based on microseismic information fractal dimensions was constructed, and the performances of deep learning models such as BP, SVM, PSO-SVM and PSO-BP under this framework were compared. Through a specific case study, the prediction results in the study area are compared with the actual results, and the reliability of the research results was verified. The following conclusions can be drawn:

1. The microseismic monitoring results in the mined area were calculated by the fractal dimensions method and converted into the classification results of CBR. This method can solve the problem of insufficient training samples in coal burst scenarios. Under the DLFR, the accuracy of the PSO-SVM and PSO-BP models reached 86.61% and 82.21%, respectively. The CBR can be effectively identified using the DLFR proposed in this paper.
2. In the deep learning model, the effect of the deep learning structure optimized by the PSO algorithm is significantly better than that of the ordinary deep learning structure. The PSO method ensures the convergence and accuracy of deep learning and improves the convergence speed.
3. Coal burst phenomenon areas and high-energy microseismic events mostly occur in high dangerous area, with this, different pressure relief measures can be formulated for different CBR levels based on the results of the deep learning predictions to achieve "graded" precise prevention and control.
4. Based on the PSO-SVM model, the results show that the highly dangerous areas of coal bursts mainly occur in areas with large MD, high W, large LPC, and high GSD.

Availability of data and materials The datasets used and/or analyzed during the current study are available from the corresponding author on reasonable request.

Declarations

Ethics approval and consent to participate Not applicable.

Consent for publication All authors have read and agreed to the published version of the manuscript.

Competing interests The authors declare that they have no known competing financial interests or personal relationships that could have appeared to influence the work reported in this paper.

References

Arndt S, Turvey C, Andreasen NC (1999) Correlating and predicting psychiatric symptom ratings: Spearmans r versus Kendall's tau correlation. J Psychiatr Res 33:97–104. https://doi.org/10.1016/S0022-3956(98)90046-2

Borisov KI, Gorshkov LK, Sofin AP, Fedorova LA (2019) Natural-technological disasters as manifestations of geodynamic instability of the Earth's crust. Bull Tomsk Polytech Univ-Geo Assets Eng 330:126–133. https://doi.org/10.18799/24131830/2019/6/2134

Bukowska M (2006) The probability of rockburst occurrence in the Upper Silesian Coal Basin area dependent on natural mining conditions. J Min Sci 42:570–577. https://doi.org/10.1007/s10913-006-0101-0

Cai W, Bai XX, Si GY, Cao WZ, Gong SY, Dou LM (2020) A monitoring investigation into rock burst mechanism based on the coupled theory of static and dynamic stresses. Rock Mech Rock Eng 53:5451–5471. https://doi.org/10.1007/s00603-020-02237-6

Cao JR, Dou LM, Konietzky H, Zhou KY, Zhang M (2023) Failure mechanism and control of the coal bursts triggered by mining-induced seismicity: a case study. Environ Earth Sci. https://doi.org/10.1007/s12665-023-10856-9

Cheng XG, Qiao W, Dou LM, He H, Ju W, Zhang JK, Song SK, Cui H, Fang HZ (2023) In-situ stress field inversion and its impact on mining-induced seismicity. Geomat Nat Hazards Risk 14:176–195. https://doi.org/10.1080/19475705.2022.2158377

Cherkassky V, Ma Y (2004) Practical selection of SVM parameters and noise estimation for SVM regression. Neural Netw 17:113–126. https://doi.org/10.1016/S0893-6080(03)00169-2

Dai LP, Pan YS, Zhang CG, Wang AW, Canbulat I, Shi TW, Wei CC, Cai RH, Liu FY, Gao XP (2022) New criterion of critical mining stress index for risk evaluation of roadway rockburst. Rock Mech Rock Eng 55:4783–4799. https://doi.org/10.1007/s00603-022-02888-7

Dao DV, Jaafari A, Bayat M, Mafi-Gholami D, Qi C, Moayedi H et al (2020) A spatially explicit deep learning neural network model for the prediction of landslide susceptibility. Catena (amst) 188:104451. https://doi.org/10.1016/j.catena.2019.104451

Dou LM, He XQ (2002) Mining geophysics. China Science and Culture Press, Xuzhou

Dou LM, Cai W, Cao AY, Guo WH (2018) Comprehensive early warning of rock burst utilizing microseismic multi-parameter indices. Int J Min Sci Technol 28:767–774. https://doi.org/10.1016/j.ijmst.2018.08.007

Dou DY, Zhou DY, Yang JG, Zhang Y (2020) Coal and gangue recognition under four operating conditions by using image analysis and Relief-SVM. Int J Coal Prep Util 40:473–482. https://doi.org/10.1080/19392699.2018.1540416

Dou LM, Tian XY, Cao AY, Gong SY, He H, He J, Cai W, Li XW (2022) Present situation and problems of coal mine rock burst prevention and control in China. J China Coal Soc 47(1):152–171. https://doi.org/10.13225/j.cnki.jccs.YG21.1873

Du WS, Li HT, Qi QX, Zheng WY, Yang SS (2022) Research on multi-factor analysis and quantitative evaluation method of rockburst risk in coal mines. Lithosphere. https://doi.org/10.2113/2022/5005317

Duan Y, Shen YR, Canbulat I, Luo X, Si GY (2021) Classification of clustered microseismic events in a coal mine using machine learning. J Rock Mech Geotech Eng 13(6):1256–1273. https://doi.org/10.1016/j.jrmge.2021.09.002

Han Y, Wang Q, Li W, Yang Z, Gu T, Wang Z (2023) Predicting the height of the water-conducting fractured zone in fully mechanized top coal caving longwall mining of very thick jurassic coal seams in western China based on the NNBR model. Mine Water Environ 42:121–133. https://doi.org/10.1007/s10230-023-00918-6

Jiang BY, Wang LG, Lu YL, Wang CQ, Ma D (2016) Combined early warning method for rockburst in a Deep

Island, fully mechanized caving face. Arab J Geosci. https://doi.org/10.1007/s12517-016-2776-0

Kan JL, Dou LM, Li XW, Cao JR, Bai JZ, Chai YJ (2022) Study on influencing factors and prediction of peak particle velocity induced by roof pre-split blasting in underground. Undergr Space 7:1068–1085. https://doi.org/10.1016/j.undsp.2022.02.002

King G (1983) The accommodation of large strains in the upper lithosphere of the Earth and other solids by self-similar fault systems; the geometrical origin of b-value. Pure Appl Geophys 121:761–815. https://doi.org/10.1007/BF02590182

Konicek P, Schreiber J (2018) Heavy rockbursts due to long-wall mining near protective pillars: a case study. Int J Min Sci Technol 28:799–805. https://doi.org/10.1016/j.ijmst.2018.08.010

Kuang TJ, Li Z, Zhu WB, Xie JL, Ju JF, Liu JR, Xu JM (2019) The impact of key strata movement on ground pressure behaviour in the Datong coalfield. Int J Rock Mech Min Sci 119:193–204. https://doi.org/10.1016/j.ijrmms.2019.04.010

Li Q, Wei W (2021) AVO inversion in orthotropic media based on SA-PSO. IEEE Trans Geosci Remote Sens 59:8903–8912. https://doi.org/10.1109/TGRS.2021.3053044

Liu QZ, Chen CH, Zhang Y, Hu ZG (2011) Feature selection for support vector machines with RBF kernel. Artif Intell Rev 36:99–115. https://doi.org/10.1007/s10462-011-9205-2

Liu WY, Piao CD, Zhou YZ, Zhao CQ (2021) Predictive model of overburden deformation: based on machine learning and distributed optical fiber sensing technology. Eng Comput (swansea) 38:2207–2227. https://doi.org/10.1108/EC-05-2020-0281

Ma ZJ, Mei G (2021) Deep learning for geological hazards analysis: Data, models, applications, and opportunities. Earth Sci Rev. https://doi.org/10.1016/j.earscirev.2021.103858

Newman C, Newman D (2021) Numerical analysis for the prediction of bump prone conditions: a southern Appalachian pillar coal bump case study. Int J Min Sci Technol 31:75–81. https://doi.org/10.1016/j.ijmst.2020.12.020

Peng YW, Qi QX, Mao DB, Ren Y (2010) Research on evaluation method for coal bursting danger in coal mining. Coal Min Technol 15(1):1–3+7. https://doi.org/10.3969/j.issn.1006-6225.2010.01.002

Polson N, Sokolov V (2020) Deep learning: computational aspects. Wiley Interdiscip Rev Comput Stat. https://doi.org/10.1002/wics.1500

Qi QX, Li YZ, Zhao SK, Zhang NB, Zheng WY, Li HT, Li HY (2019) Seventy years development of coal mine rockburst in China: establishment and consideration of theory and technology system. Coal Sci Technol 47(9):1–40. https://doi.org/10.13199/j.cnki.cst.2019.09.001

Qiao W, Li WP, Zhang X, Niu YF, Chen YK, Wang YZ, Tao X (2019) Prediction of floor water disasters based on fractal analysis of geologic structure and vulnerability index method for deep coal mining in the Yanzhou mining area. Geomat Nat Hazards Risk 10:1306–1326. https://doi.org/10.1080/19475705.2019.1574911

Sharma T, Kaur K (2021) Benchmarking deep learning methods for aspect level sentiment classification. Appl Sci (basel). https://doi.org/10.3390/app112210542

Shen F, Zhang X, Wang R, Lan D, Zhou W (2022) Sequential optimization three-way decision model with information gain for credit default risk evaluation. Int J Forecast 38:1116–1128. https://doi.org/10.1016/j.ijforecast.2021.12.011

Si GY, Cai W, Wang SY, Li X (2020) Prediction of relatively high-energy seismic events using spatial-temporal parametrisation of mining-induced seismicity. Rock Mech Rock Eng 53:5111–5132. https://doi.org/10.1007/s00603-020-02210-3

Sun WC, Zhang P, Wei HJ, Miao CY, Zhao K (2015) Optimization of vacuum hybrid welding process parameters for YG8 cemented carbide and 42CrMo steel using artificial neural networks. Mater Trans 56:1179–1185. https://doi.org/10.2320/matertrans.M2015003

Sun YT, Li GC, Zhang JF, Huang JD (2021) Rockburst intensity evaluation by a novel systematic and evolved approach: machine learning booster and application. Bull Eng Geol Environ 80:8385–8395. https://doi.org/10.1007/s10064-021-02460-7

Turcotte DL (1986) A fractal model for crustal deformation. Tectonophysics 132:261–269. https://doi.org/10.1016/0040-1951(86)90036-3

Velandia F, Bermúdez MA (2018) The transpressive southern termination of the Bucaramanga fault (Colombia): insights from geological mapping, stress tensors, and fractal analysis. J Struct Geol 115:190–207. https://doi.org/10.1016/j.jsg.2018.07.020

Wang YF, Cui F (2018) Energy evolution mechanism in process of Sandstone failure and energy strength criterion. J Appl Geophys 154:21–28. https://doi.org/10.1016/j.jappgeo.2018.04.025

Wang SY, Si GY, Wang CB, Cai W, Li BL, Oh J, Canbulat I (2022) Quantitative assessment of the spatio-temporal correlations of seismic events induced by longwall coal mining. J Rock Mech Geotech Eng 14(5):1406–1420. https://doi.org/10.1016/j.jrmge.2022.04.002

Wu AY, Yao J, Xiao HF (2005) Optimization for prediction index of coal and gas outburst based on gray associated analysis. Coal Sci Technol 33:55–58. https://doi.org/10.13199/j.cst.2005.04.58.wuay.017

Wu M, Ye YC, Wang QH, Hu NY (2022) Development of rockburst research: a comprehensive review. Appl Sci (basel). https://doi.org/10.3390/app12030974

Wu W, Zhou Y, Wei HX (2013) A fault diagnosis of suck rod pumping system based on SVM. In: Gao S, ed. Mechatronics and computational mechanics. International conference on mechatronics and computational mechanics (ICMCM 2012) 307, pp 285–9. https://doi.org/10.4028/www.scientific.net/AMM.307.285

Yan J, Li L (2013) Multi-objective optimization of milling parameters—the trade-offs between energy, production rate and cutting quality. J Clean Prod 52:462–471. https://doi.org/10.1016/j.jclepro.2013.02.030

Yang N, Wang R, Liu Z, Yao Z (2023) Landslide susceptibility prediction improvements based on a semi-integrated

supervised machine learning model. Environ Sci Pollut Res Int 30:50280–50294. https://doi.org/10.1007/s11356-023-25650-0

Yao J, Qin S, Qiao S, Liu X, Zhang L, Chen J (2022) Application of a two-step sampling strategy based on deep neural network for landslide susceptibility mapping. Bull Eng Geol Environ. https://doi.org/10.1007/s10064-022-02615-0

Zhang CQ, Yu J, Chen J, Lu JJ (2016a) Zhou H (2016) Evaluation method for potential rockburst in underground engineering. Rock Soil Mech 37:341–349. https://doi.org/10.16285/j.rsm.2016.S1.046

Zhang HW, Meng QN, Han J, Tang GY, Zhu F (2016b) Application of the geological dynamic division in rock burst coal mine. J Liaoning Tech Univ (natl Sci) 35(5):449–455. https://doi.org/10.11956/j.issn.1008-0562.2016.05.001

Zhang J, Cheng X, Qiao W, Lv W, He H, Dou L et al (2022) Risk assessment of rockburst with a LS-FAHP-CRITIC method: a case in Gaojiapu Coal Mine, North of China. Geofluids 2022:1–13. https://doi.org/10.1155/2022/7275050

Zhao ZG, Zhang CJ, Gou XF, Sang HT (2015) Solar cell temperature prediction model of support vector machine optimized by particle swarm optimization algorithm. Acta Phys Sin. https://doi.org/10.7498/aps.64.088801

Zhou KY, Dou LM, Gong SY, Li JZ, Zhang JK, Cao JR (2020) Study of rock burst risk evolution in front of deep longwall panel based on passive seismic velocity tomography. Geofluids. https://doi.org/10.1155/2020/8888413

Zhou B, Xu J, Peng SJ, Yan FZ, Yang W, Cheng L, Ni GH (2022) Influence of geo-stress on dynamic response characteristics of coal and gas outburst. Rock Mech Rock Eng 53:4819–4837. https://doi.org/10.1007/s00603-020-02154-8

Zhu ZJ, Zhang HW, Han J, Lv YC (2018) A risk assessment method for rockburst based on geodynamic environment. Shock Vib. https://doi.org/10.1155/2018/2586842

Publisher's Note   Springer Nature remains neutral with regard to jurisdictional claims in published maps and institutional affiliations.